


Analysis of $\Omega(212)$ as a molecule in the chiral quark model

Xiaohuang Hu and Jialun Ping 

Department of Physics and Jiangsu Key Laboratory for Numerical Simulation of Large Scale Complex Systems, Nanjing Normal University, Nanjing 210023, People's Republic of China

 (Received 21 July 2022; accepted 13 September 2022; published 26 September 2022)

Inspired by the updated information on $\Omega(212)$ by the Belle Collaboration, we conduct a study of all possible S -wave pentaquark systems with quark contents $sss\bar{q}\bar{q}$, $q = u, d$ in a chiral quark model with the help of Gaussian expansion method. Channel coupling is also considered. The real-scaling method (stabilization method) is employed to identify and check the bound states and the genuine resonances. In addition, the decay widths of all resonances are given. The results show that $\Omega(212)$ can be interpreted as a $\Xi^* \bar{K}$ molecular state with quantum number of $IJ^P = 0(\frac{3}{2})^-$. Another bound state $\Omega\pi$ with $IJ^P = 1(\frac{3}{2})^-$ is also found. Other resonances are obtained: $\Xi^* \bar{K}^*$ with $IJ^P = 0(\frac{1}{2})^-$ and $0(\frac{3}{2})^-$. These pentaquark states is expected to be further verified in future experiments.

DOI: [10.1103/PhysRevD.106.054028](https://doi.org/10.1103/PhysRevD.106.054028)

I. INTRODUCTION

In 2018, an excited state of Ω with a significance of 8.6σ was reported in the $K^-\Xi^0$ and $K_S^0\Xi^-$ invariant mass distributions by the Belle Collaboration [1]. The measured mass and width of the state are $2012.4 \pm 0.7 \pm 0.6$ MeV and $6.4^{+2.5}_{-2.0} \pm 1.6$ MeV, respectively. Although the ground state $\Omega(1672)$ was predicted in the quark model with the SU(3)-flavor symmetry by Gell-Mann [2] and Ne'eman [3] and discovered experimentally in 1960s, only three Ω excited states were listed in the Particle Data Group before the observation by the Belle Collaboration and there was little knowledge of the nature of them. Thus, the discovery of $\Omega(212)$ was very welcome and triggered many theoretical investigations on the nature of the excited states of Ω .

Before the observation of the state $\Omega(212)$, a series of theoretical models and approaches, such as the quark model [4,5], Skyrme model [6], lattice QCD [7], and large N_c [8], predicted that the masses of the first excited states of the $\Omega(1672)$ are around 2.0 GeV, which are consistent with the result of the Belle Collaboration. Thus, it is reasonable to explain the $\Omega(212)$ as a good candidate for the first orbital excited state of $\Omega(1672)$. After the observation of $\Omega(212)$, the subsequent theoretical researches have further explored the qqq picture of $\Omega(212)$ in the chiral quark model [9], QCD sum rule [10], and 3P_0 model [11].

Nevertheless, the possibility of the pentaquark picture of $\Omega(212)$ cannot be excluded, considering its mass is very close to the threshold of the state $\Xi^* \bar{K}$. Actually, various theoretical approaches [12–15] have investigated the Ω excited states in pentaquark picture before the Belle Collaborations's report. The observation of the $\Omega(212)$ also triggered a lot of theoretical work on this issue. In Ref. [16] the flavor SU(3) analysis was performed and it was found that the $\Omega(212)$ is likely to be a $\Xi^* \bar{K}$ molecular state with $J^P = \frac{3}{2}^-$. Several works also interpreted $\Omega(212)$ as a possible $\Xi^* \bar{K}$ molecular state and further predicted a large decay width for the $\Omega(212) \rightarrow \Xi^* \bar{K} \rightarrow \Xi\pi\bar{K}$ [17–20]. In Ref. [21], the $\Omega(212)$ was a dynamically generated state from the coupled channel interactions of $\Xi^* \bar{K}$ and $\Omega\eta$ in S wave. Inspired by these theoretical results, a follow-up experiment was reported by the Belle Collaboration to measure three body decay of the $\Omega(212)$ to $\Xi\pi\bar{K}$ [22]. The result showed that there are no significant $\Omega(212)$ signals in the $\Xi\pi\bar{K}$ channel, which was in tension with the molecular interpretation of the $\Omega(212)$. Based on the measurements, Refs. [23,24] revisited the $\Omega(212)$ using the coupled channel unitary approach in the molecular perspective, taking account of the interaction of the $\Xi^* \bar{K}$, $\Omega\eta$, and $\Xi\bar{K}$ (D-wave) channels and indicated that the experimental properties of $\Omega(212)$ [22] can be easily accommodated. In the hadronic molecular approach, the state $\Omega(212)$ can be interpreted as the P -wave $\Xi^* \bar{K}$ molecule state with $IJ^P = 0(\frac{1}{2})^+$ or $\frac{3}{2}^+$ [25], while in Ref. [26], the $\Omega(212)$ was considered to contain the mixed $\Xi^* \bar{K}$ and $\Omega\eta$ hadronic components. In Ref. [27], a nonrelativistic constituent quark potential model was used and $\Omega(212)$ can be interpreted as a P -wave state with $J^P = \frac{3}{2}^-$ in qqq picture. In Ref. [28], the $\Omega(212)$ was

Published by the American Physical Society under the terms of the [Creative Commons Attribution 4.0 International license](https://creativecommons.org/licenses/by/4.0/). Further distribution of this work must maintain attribution to the author(s) and the published article's title, journal citation, and DOI. Funded by SCOAP³.

study in the nonleptonic weak decays of $\Omega_c^0 \rightarrow \Xi^* \bar{K} \pi^+ (\Omega \eta) \rightarrow (\Xi \bar{K})^- \pi^+$ and $(\Xi \bar{K} \pi)^- \pi^+$ via final-state interactions of the $\Xi^* \bar{K}$ and $\Omega \eta$ pairs. However, the Belle Collaboration has revisited the measurement of $\Omega(2012)^- \rightarrow \Xi(1530)^0 K^- \rightarrow \Xi^- \pi^+ K^-$ and updated the measurements of $\Omega(2012)^- \rightarrow \Xi^0 K^-$ and $\Omega(2012)^- \rightarrow \Xi^- K_S^0$ with improved selection criteria very recently [29]. The results show that the ratio of the branching fraction for the resonant three-body decay to that for the two-body decay to $\Xi \bar{K}$ is $0.97 \pm 0.24 \pm 0.07$, consistent with the molecular picture of $\Omega(2012)$. The conclusion is in contrast to the previous study [22] and suggests that $\Omega(2012)$ can be interpreted as a molecular state.

The state $\Omega(2012)$ was also investigated in the framework of chiral quark model (ChQM) and quark delocalization color screening model (QDCSM) before in our group [30]. However, there is a mass inversion of $\Xi^* \bar{K}$ channel and $\Omega \eta$ channel due to the single Gaussian approximation in constructing the wave functions of hadrons. In the Rayleigh-Ritz variational method, the basis expansion of the trial wave function is significant. In this work, Gaussian expansion method (GEM) [31] in which each relative motion in the system is expanded in terms of Gaussian basis functions whose sizes are taken in geometric progression, is adopted. The GEM has proven to be an accurate and universal few-body calculation method [32–35] and we hope to solve the previous problem of mass inversion using this method, and to describe the hadron spectrum better. The constituent chiral quark model will still be employed to investigate all possible S -wave pentaquark systems for $\Omega(2012)$, considering the channel-coupling interactions. After considering all possible configurations of color, spin, and flavor degrees of freedom, we can identify the structures of these systems. Finally, with the help of “real scaling method” [36–38], we can confirm the bound states and the genuine resonances and obtain decay widths of resonances.

The paper is organized as follows. After introduction, details of ChQM and GEM are introduced in Sec. II. In Sec. III, we present the numerical results and a method of finding and calculating decay widths of genuine resonance states (“real scaling method”). Finally, we give a brief summary of this work in the last section.

II. CHIRAL QUARK MODEL AND WAVE FUNCTIONS

When it comes to multi-quark candidates observed by experiments, the QCD-inspired quark model approach is still one of the most common tools for describing them. The chiral quark model has become one of the most effective approaches to describe hadron spectra,

hadron-hadron interactions, and multi-quark states [39]. The general form of five-body Hamiltonian in the model is given as follows:

$$H = \sum_{i=1}^5 \left(m_i + \frac{p_i^2}{2m_i} \right) - T_{CM} + \sum_{j>i=1}^5 [V_{\text{CON}}(\mathbf{r}_{ij}) + V_{\text{OGE}}(\mathbf{r}_{ij}) + V_{\text{GBE}}(\mathbf{r}_{ij})], \quad (1)$$

where m_i is the constituent mass of quark (antiquark), \mathbf{p}_i is momentum of quark, and T_{cm} is the kinetic energy of the center-of-mass motion. Due to the fact that a nearly massless current light quark acquires a dynamical, momentum dependent mass (so-called constituent quark mass) for its interaction with the gluon medium, ChQM contains color confinement potential, one-gluon exchange potential (OGE), and Goldstone boson exchange potentials (GBE). These three potentials reveal the most relevant features of QCD at the low-energy regime; confinement, asymptotic freedom, and chiral symmetry spontaneous breaking.

In this work, we are interested in the low-lying pentaquark systems of S -waves composed of $sss\bar{q}q$, $q = u, d$. Hence, only the central part of the quark-quark interactions are considered. For color confinement potential, the screened form is used,

$$V_{\text{CON}}(\mathbf{r}_{ij}) = \lambda_i^c \cdot \lambda_j^c [-a_c (1 - e^{-\mu_c r_{ij}}) + \Delta], \quad (2)$$

where a_c , μ_c , and Δ are model parameters, and λ^c represent the SU(3) color Gell-Mann matrices.

One-gluon exchange potential contains so-called coulomb and color-magnetism interactions, which arise from QCD perturbation effects,

$$V_{\text{OGE}}(\mathbf{r}_{ij}) = \frac{1}{4} \alpha_s \lambda_i^c \cdot \lambda_j^c \left[\frac{\boldsymbol{\sigma}_i \cdot \boldsymbol{\sigma}_j}{r_{ij}} - \frac{1}{6m_i m_j} \frac{e^{-r_{ij}/r_0(\mu)}}{r_{ij} r_0^2(\mu)} \right], \quad (3)$$

where μ is the reduced mass between two interacting quarks, $\boldsymbol{\sigma}$ represents the SU(2) Pauli matrices, $r_0(\mu) = \hat{r}_0/\mu$, and α_s denotes the effective scale-dependent strong running coupling constant of one-gluon exchange,

$$\alpha_s = \frac{\alpha_0}{\ln\left(\frac{\mu^2 + \mu_0^2}{\Lambda_0^2}\right)}. \quad (4)$$

Due to chiral symmetry spontaneous breaking, Goldstone boson exchange potentials appear between light quarks (u, d and s),

$$\begin{aligned}
V_{GBE}(\mathbf{r}_{ij}) &= V_\pi(\mathbf{r}_{ij}) + V_K(\mathbf{r}_{ij}) + V_\eta(\mathbf{r}_{ij}) + V_{sc}(\mathbf{r}_{ij}), \\
V_\pi(\mathbf{r}_{ij}) &= \frac{g_{ch}^2}{4\pi} \frac{m_\pi^2}{12m_i m_j} \frac{\Lambda_\pi^2 m_\pi}{\Lambda_\pi^2 - m_\pi^2} \left[Y(m_\pi r_{ij}) - \frac{\Lambda_\pi^3}{m_\pi^3} Y(\Lambda_\pi r_{ij}) \right] (\boldsymbol{\sigma}_i \cdot \boldsymbol{\sigma}_j) \sum_{a=1}^3 \lambda_i^a \lambda_j^a, \\
V_K(\mathbf{r}_{ij}) &= \frac{g_{ch}^2}{4\pi} \frac{m_K^2}{12m_i m_j} \frac{\Lambda_K^2 m_K}{\Lambda_K^2 - m_K^2} \left[Y(m_K r_{ij}) - \frac{\Lambda_K^3}{m_K^3} Y(\Lambda_K r_{ij}) \right] (\boldsymbol{\sigma}_i \cdot \boldsymbol{\sigma}_j) \sum_{a=4}^7 \lambda_i^a \lambda_j^a, \\
V_\eta(\mathbf{r}_{ij}) &= \frac{g_{ch}^2}{4\pi} \frac{m_\eta^2}{12m_i m_j} \frac{\Lambda_\eta^2 m_\eta}{\Lambda_\eta^2 - m_\eta^2} \left[Y(m_\eta r_{ij}) - \frac{\Lambda_\eta^3}{m_\eta^3} Y(\Lambda_\eta r_{ij}) \right] (\boldsymbol{\sigma}_i \cdot \boldsymbol{\sigma}_j) [\cos \theta_P (\lambda_i^8 \lambda_j^8) - \sin \theta_P (\lambda_i^0 \lambda_j^0)], \quad (5)
\end{aligned}$$

where $Y(x)$ is the standard Yukawa functions, λ^a are the $SU(3)$ flavor Gell-Mann matrices, Λ are the cutoffs, m_χ , $\chi = \pi, K, \eta$ are the masses of Goldstone bosons, and g_{ch}^2 is the chiral field coupling constant, which is determined from the $NN\pi$ coupling constant through

$$\frac{g_{ch}^2}{4\pi} = \frac{9}{25} \frac{g_{\pi NN}^2}{4\pi} \frac{m_{u,d}^2}{m_N^2}. \quad (6)$$

Additionally, the scalar nonet (the extension of chiral partner σ meson) exchange V_{sc} is also used in this work, which introduces other higher multipion terms that are simulated through the full nonet of scalar mesons exchange between two constituent quarks [40].

$$\begin{aligned}
V_{sc}(\mathbf{r}_{ij}) &= V_{a_0}(\mathbf{r}_{ij}) \sum_{a=1}^3 \lambda_i^a \lambda_j^a + V_\kappa(\mathbf{r}_{ij}) \sum_{a=4}^7 \lambda_i^a \lambda_j^a \\
&\quad + V_{f_0}(\mathbf{r}_{ij}) \lambda_i^8 \lambda_j^8 + V_\sigma(\mathbf{r}_{ij}) \lambda_i^0 \lambda_j^0, \\
V_s(\mathbf{r}_{ij}) &= -\frac{g_{ch}^2}{4\pi} \frac{\Lambda_s^2 m_s}{\Lambda_s^2 - m_s^2} \left[Y(m_s r_{ij}) - \frac{\Lambda_s}{m_s} Y(\Lambda_s r_{ij}) \right], \\
s &= a_0, \kappa, f_0, \sigma. \quad (7)
\end{aligned}$$

The model parameters are listed in Table I, and the calculated baryon and meson masses are presented in Table II along with the experimental values. Because it is difficult to use the same set of parameters to obtain a good description of baryon and meson spectra simultaneously, we treat the strong coupling constant of the one-gluon exchange with different values for quark-quark and quark-antiquark interacting pairs. From the calculation, most of the results are close to experimental values except for ω . In the follow-up calculation, we find that the molecular states consisting of this meson are open channels, and these channels have no effect on all stable molecular states so these errors do not affect our final results.

In the following, the wave functions for the pentaquark systems are constructed and the eigenenergy is obtained by solving the Schrödinger equation. The wave function of the system consists of four parts; orbital, spin, flavor, and color. The wave function of each part is constructed in two steps; first construct the wave function of three-quark cluster and quark-antiquark cluster, respectively, then coupling

two-cluster wave functions to form the complete five-body one. In this work, the wave functions for the $(ssq)(\bar{q}s)$ configuration is written down, and the wave functions for other configurations can be obtained by exchange the indices of particles. The indices of particles s, s, q, \bar{q}, s are 1,2,3,4,5.

TABLE I. Quark model parameters.

Quark masses	$m_u = m_d$ (MeV)	313
	m_s (MeV)	555
Goldstone bosons	Λ_π (fm $^{-1}$)	4.20
	$\Lambda_\eta = \Lambda_K$ (fm $^{-1}$)	5.20
	m_π (fm $^{-1}$)	0.70
	m_K (fm $^{-1}$)	2.51
	m_η (fm $^{-1}$)	2.77
	$g_{ch}^2/(4\pi)$	0.54
	θ_P ($^\circ$)	-15
Confinement	a_c (MeV)	465.3
	μ_c (fm $^{-1}$)	0.58
	Δ (MeV)	164.52
Scalar nonet	m_σ (fm $^{-1}$)	3.42
	Λ_σ (fm $^{-1}$)	4.20
	$\Lambda_{a_0} = \Lambda_\kappa = \Lambda_{f_0}$ (fm $^{-1}$)	5.20
	$m_{a_0} = m_\kappa = m_{f_0}$ (fm $^{-1}$)	4.97
OGE	\hat{r}_0 (MeV fm)	35.19
	α_{uu}	0.467/0.662
	α_{us}	0.695/0.573
	α_{ss}	0.29/0.335

TABLE II. The masses of ground-state baryons and mesons (MeV).

	Λ	Σ	Σ^*	Ξ	Ξ^*	Ω
CHQM	1115	1191	1392	1318	1537	1672
Expt	1116	1189	1386	1315	1530	1672
	π	ρ	\bar{K}	\bar{K}^*	η'	ϕ
CHQM	139	768	498	915	958	1048
Expt	140	775	498	892	958	1020
	η	ω				
CHQM	560	590				
Expt	548	782				

As an example the wave functions for $(sss)(\bar{q}q)$ are obtained by exchanging the particle indices $3 \leftrightarrow 5$.

The first part is an orbital wave function. A five-body system has four relative motions so it is written as follows:

$$\psi_{LM_L}^x = [[\psi_{n_1 l_1}(\boldsymbol{\rho}) \psi_{n_2 l_2}(\boldsymbol{\lambda})]_l \psi_{n_3 l_3}(\mathbf{r})]_{l'} \psi_{n_4 l_4}(\mathbf{R})]_{LM_L}, \quad (8)$$

where the Jacobi coordinates are defined as follows:

$$\begin{aligned} \boldsymbol{\rho} &= \mathbf{x}_1 - \mathbf{x}_2, \\ \boldsymbol{\lambda} &= \left(\frac{m_1 \mathbf{x}_1 + m_2 \mathbf{x}_2}{m_1 + m_2} \right) - \mathbf{x}_3, \\ \mathbf{r} &= \mathbf{x}_4 - \mathbf{x}_5, \\ \mathbf{R} &= \left(\frac{m_1 \mathbf{x}_1 + m_2 \mathbf{x}_2 + m_3 \mathbf{x}_3}{m_1 + m_2 + m_3} \right) - \left(\frac{m_4 \mathbf{x}_4 + m_5 \mathbf{x}_5}{m_4 + m_5} \right). \end{aligned} \quad (9)$$

\mathbf{x}_i is the position of the i th particle. Then we use a set of Gaussians to expand the radial part of the orbital wave function which is shown below,

$$\psi_{lm}(\mathbf{r}) = \sum_{n=1}^{n_{\max}} c_{nl} \phi_{nlm}^G(\mathbf{r}), \quad (10)$$

$$\phi_{nlm}^G(\mathbf{r}) = N_{nl} r^l e^{-\nu_n r^2} Y_{lm}(\hat{\mathbf{r}}), \quad (11)$$

where N_{nl} is the normalization constant,

$$N_{nl} = \left(\frac{2^{l+2} (2\nu_n)^{l+3/2}}{\sqrt{\pi} (2l+1)!!} \right)^{\frac{1}{2}}, \quad (12)$$

and c_{nl} is the variational parameter, which is determined by the dynamics of the system. The Gaussian-size parameters are chosen according to the following geometric progression,

$$\nu_n = \frac{1}{r_n^2}, \quad r_n = r_{\min} a^{n-1}, \quad a = \left(\frac{r_{\max}}{r_{\min}} \right)^{\frac{1}{n_{\max}-1}}, \quad (13)$$

where n_{\max} is the number of Gaussian functions, and n_{\max} is determined by the convergence of the results. In the present calculation, $n_{\max} = 8$ and the results of calculation tends to be stable.

Considering the quark content of pentaquark systems is $sss\bar{q}q$, $q = u, d$, there are two flavor configurations, $(ssq)(\bar{q}s)$ and $(sss)(\bar{q}q)$. Based on the flavor SU(2) symmetry, due to the mass difference between s quark and u, d quarks, the flavor wave functions of three-quark and quark-antiquark subclusters can be constructed as follows:

$$\begin{aligned} |B_{\frac{3}{2}, \frac{1}{2}}\rangle &= ssu, |B_{\frac{3}{2}, -\frac{1}{2}}\rangle = ssd, \\ |B_{0,0}\rangle &= sss, \\ |M_{\frac{1}{2}, \frac{1}{2}}\rangle &= \bar{d}s, |M_{\frac{1}{2}, -\frac{1}{2}}\rangle = -\bar{u}s, \\ |M_{1,1}\rangle &= u\bar{d}, |M_{1,0}\rangle = \frac{1}{\sqrt{2}}(-\bar{u}u + \bar{d}d), |M_{1,-1}\rangle = -\bar{u}d, \\ |M_{0,0}\rangle &= \frac{1}{\sqrt{2}}(-\bar{u}u - \bar{d}d). \end{aligned} \quad (14)$$

The possible isospin quantum numbers for the pentaquark systems under the present investigation are 0 and 1. Then the flavor wave functions for pentaquark systems in two configurations can be obtained by coupling with help of Clebsch-Gordan coefficients as follows:

$$\begin{aligned} |\chi_{0,0}^{f1}\rangle &= \frac{1}{\sqrt{2}} |B_{\frac{3}{2}, \frac{1}{2}}\rangle |M_{\frac{1}{2}, -\frac{1}{2}}\rangle - \frac{1}{\sqrt{2}} |B_{\frac{3}{2}, -\frac{1}{2}}\rangle |M_{\frac{1}{2}, \frac{1}{2}}\rangle, \\ |\chi_{0,0}^{f2}\rangle &= |B_{0,0}\rangle |M_{0,0}\rangle, \\ |\chi_{0,0}^{f3}\rangle &= |B_{\frac{3}{2}, \frac{1}{2}}\rangle |M_{\frac{1}{2}, \frac{1}{2}}\rangle, \\ |\chi_{0,0}^{f4}\rangle &= |B_{0,0}\rangle |M_{1,1}\rangle. \end{aligned} \quad (15)$$

The details of constructing color and spin wave functions of pentaquark systems can be found in Ref. [32], and only the last expressions are shown here.

Color wave functions:

$$\begin{aligned} |\chi^{c1}\rangle &= \frac{1}{\sqrt{18}} (rgb - rbg + gbr - grb + brg - bgr)(\bar{r}r + \bar{g}g + \bar{b}b), \\ |\chi^{c2}\rangle &= \frac{1}{\sqrt{192}} [2(2rrg - rgr - grr)\bar{r}b + 2(rgg + grg - 2ggr)\bar{g}b - 2(2rrb - rbr - brr)\bar{r}g - 2(rbb + brb - 2bbr)\bar{b}g \\ &\quad + 2(2ggb - gbg - bgg)\bar{g}r + 2(gbb + bgb - 2bbg)\bar{b}r + (rbg - gbr + brg - bgr)(2\bar{b}b - \bar{r}r - \bar{g}g) \\ &\quad + (2rgb - rbg + 2grb - gbr - brg - bgr)(\bar{r}r - \bar{g}g)], \\ |\chi^{c3}\rangle &= \frac{1}{24} [6(rgr - grr)\bar{r}b + 6(rgg - grg)\bar{g}b - 6(rbr - brr)\bar{r}g - 6(rbb - brb)\bar{b}g + 6(gbg - bgg)\bar{g}r + 6(gbb - bgb)\bar{b}r \\ &\quad + 3(rbg + gbr - brg - bgr)(\bar{r}r - \bar{g}g) + (2rgb + rbg - 2grb - gbr - brg + bgr)(2\bar{b}b - \bar{r}r - \bar{g}g)]. \end{aligned} \quad (16)$$

Spin wave functions:

$$\begin{aligned}
|\chi_{\frac{1}{2},\frac{1}{2}}^{\sigma 1}\rangle &= \frac{1}{\sqrt{12}}(2\alpha\alpha\beta\alpha\beta - 2\alpha\alpha\beta\beta\alpha + \alpha\beta\alpha\beta\alpha \\
&\quad - \alpha\beta\alpha\alpha\beta + \beta\alpha\alpha\beta\alpha - \beta\alpha\alpha\alpha\beta), \\
|\chi_{\frac{1}{2},\frac{1}{2}}^{\sigma 2}\rangle &= \frac{1}{2}(\alpha\beta\alpha\alpha\beta - \alpha\beta\alpha\beta\alpha + \beta\alpha\alpha\beta\alpha - \beta\alpha\alpha\alpha\beta), \\
|\chi_{\frac{1}{2},\frac{1}{2}}^{\sigma 3}\rangle &= \frac{1}{6}(2\alpha\alpha\beta\alpha\beta + 2\alpha\alpha\beta\beta\alpha - \alpha\beta\alpha\alpha\beta - \alpha\beta\alpha\beta\alpha \\
&\quad - \beta\alpha\alpha\beta\alpha - \beta\alpha\alpha\alpha\beta - 2\alpha\beta\beta\alpha\alpha - 2\beta\alpha\beta\alpha\alpha + 4\beta\beta\alpha\alpha\alpha), \\
|\chi_{\frac{1}{2},\frac{1}{2}}^{\sigma 4}\rangle &= \frac{1}{\sqrt{12}}(\alpha\beta\alpha\alpha\beta + \alpha\beta\alpha\beta\alpha - \beta\alpha\alpha\alpha\beta - \beta\alpha\alpha\beta\alpha \\
&\quad + 2\beta\alpha\beta\alpha\alpha - 2\alpha\beta\beta\alpha\alpha), \\
|\chi_{\frac{1}{2},\frac{1}{2}}^{\sigma 5}\rangle &= \frac{1}{\sqrt{18}}(3\alpha\alpha\alpha\beta\beta - \alpha\alpha\beta\alpha\beta - \alpha\alpha\beta\beta\alpha \\
&\quad - \alpha\beta\alpha\alpha\beta - \alpha\beta\alpha\beta\alpha - \beta\alpha\alpha\alpha\beta - \beta\alpha\alpha\beta\alpha \\
&\quad + \beta\beta\alpha\alpha\alpha + \beta\alpha\beta\alpha\alpha + \alpha\beta\beta\alpha\alpha), \\
|\chi_{\frac{3}{2},\frac{3}{2}}^{\sigma 6}\rangle &= \frac{1}{\sqrt{6}}(2\alpha\alpha\beta\alpha\alpha - \alpha\beta\alpha\alpha\alpha - \beta\alpha\alpha\alpha\alpha), \\
|\chi_{\frac{3}{2},\frac{3}{2}}^{\sigma 7}\rangle &= \frac{1}{\sqrt{2}}(\alpha\beta\alpha\alpha\alpha - \beta\alpha\alpha\alpha\alpha), \\
|\chi_{\frac{3}{2},\frac{3}{2}}^{\sigma 8}\rangle &= \frac{1}{\sqrt{2}}(\alpha\alpha\alpha\alpha\beta - \alpha\alpha\alpha\beta\alpha), \\
|\chi_{\frac{3}{2},\frac{3}{2}}^{\sigma 9}\rangle &= \frac{1}{\sqrt{30}}(2\alpha\alpha\beta\alpha\alpha + 2\alpha\beta\alpha\alpha\alpha + 2\beta\alpha\alpha\alpha\alpha \\
&\quad - 3\alpha\alpha\alpha\alpha\beta - 3\alpha\alpha\alpha\beta\alpha), \\
|\chi_{\frac{5}{2},\frac{5}{2}}^{\sigma 10}\rangle &= \alpha\alpha\alpha\alpha\alpha, \tag{17}
\end{aligned}$$

where χ^{c1} represents the color wave function of a color singlet-singlet structure, and χ^{c2} and χ^{c3} represent the color octet-octet wave functions respectively. The subscripts of χ_{I,I_z}^f (χ_{S,S_z}^{σ}) are total isospin (spin) and its third projection.

Finally, the total wave function of the five-quark system is written as

$$\Psi_{JM_J}^{i,j,k} = \mathcal{A}[[\Psi_L \chi_S^{\sigma_i}]_{JM_J} \chi_j^f \chi_k^{ci}], \tag{18}$$

where the \mathcal{A} is the antisymmetry operator of the system which guarantees the antisymmetry of the total wave functions when identical particles exchange. Under our numbering scheme, the antisymmetry operator has the following form,

$$\mathcal{A} = 1 - (15) - (25).$$

At last, we solve the following Schrödinger equation to obtain eigenenergies of the system,

$$H\Psi_{JM_J} = E\Psi_{JM_J}, \tag{19}$$

with the help of the Rayleigh-Ritz variational principle. The matrix elements of Hamiltonian can be easily obtained if all the orbital angular momenta are zero, which is reasonable for only considering the low-lying states of pentaquark systems. It is worthwhile to mention that if the orbital-angular momenta of the systems are not zero, it is necessary to use the infinitesimally shifted Gaussian method to calculate the matrix elements [31].

III. RESULTS AND DISCUSSIONS

In this section we present the results of possible S -wave of pentaquark systems $ssq\bar{q}s$, $q = u, d$ with all possible quantum numbers $IJ^P = 0(\frac{1}{2})^-, 0(\frac{3}{2})^-, 0(\frac{5}{2})^-, 1(\frac{1}{2})^-, 1(\frac{3}{2})^-,$ and $1(\frac{5}{2})^-$. All the orbital-angular momentum of the systems are treated as zero and the corresponding parity is negative.

In Tables III–VIII, the significant calculation results are shown. In each table, columns 1 to 3 represent the indices of flavor, spin, and color wave functions in each channel. Column 4 is the corresponding physical channel of pentaquark systems. In column 5, the eigenenergy of each

TABLE III. The results for system with $IJ^P = 0\frac{1}{2}^-$. [cc1: mixing of color singlet-singlet channels, cc2: mixing of all channels (units are in MeV).]

ψ^f_i	ψ^{σ_j}	ψ^{c_k}	Channel	E	$E_{\text{th}}^{\text{Theo}}$	E_B	$E_{\text{th}}^{\text{Exp}}$	E'
$i = 1$	$j = 1$	$k = 1$	$\Xi\bar{K}$	1816	1816	0	1813	1813
$i = 1$	$j = 1, 2$	$k = 1, 2, 3$		1816				
$i = 1$	$j = 3$	$k = 1$	$\Xi\bar{K}^*$	2178	2232	-54	2207	2153
$i = 1$	$j = 3, 4$	$k = 1, 2, 3$		2166		-66		2141
$i = 1$	$j = 5$	$k = 1$	$\Xi^*\bar{K}^*$	2438	2451	-13	2422	2409
$i = 1$	$j = 5$	$k = 1, 3$		2430		-21		2401
$i = 2$	$j = 5$	$k = 1$	$\Omega\omega$	2261	2262	0	0	2454
$i = 2$	$j = 5$	$k = 1, 3$		2261				
cc1					1816	0		
cc2					1816			

TABLE IV. The results for system with $IJ^P = 1\frac{1}{2}^-$. [cc1: mixing of color singlet-singlet channels, cc2: mixing of all channels (units are in MeV).].

ψ^f_i	ψ^{σ_j}	ψ^{c_k}	Channel	E	$E_{\text{th}}^{\text{Theo}}$	E_B	$E_{\text{th}}^{\text{Exp}}$	E'
$i = 3$	$j = 1$	$k = 1$	$\Xi\bar{K}$	1816	1816	0	1813	1813
$i = 3$	$j = 1, 2$	$k = 1, 2, 3$		1816				
$i = 3$	$j = 3$	$k = 1$	$\Xi\bar{K}^*$	2220	2232	-12	2207	2195
$i = 3$	$j = 3, 4$	$k = 1, 2, 3$		2208		-24		2283
$i = 3$	$j = 5$	$k = 1$	$\Xi^*\bar{K}^*$	2431	2451	-20	2422	2402
$i = 3$	$j = 5$	$k = 1, 3$		2420		-31		2391
$i = 4$	$j = 5$	$k = 1$	$\Omega\rho$	2440	2440	0	0	2447
$i = 4$	$j = 5$	$k = 1, 3$		2440				
cc1					1816	0		
cc2					1816			

channel is listed and the theoretical threshold (the sum of the theoretical masses of corresponding baryon and meson) is given in column 6. Column 8 gives the binding energies, which are the difference between the eigenenergy and the theoretical threshold. Finally, the experimental thresholds (the sum of the experimental masses of the corresponding baryon and meson) along with corrected energies (the sum of experimental threshold and the binding energy, $E' = E_B + E_{\text{th}}^{\text{Exp}}$) are given in last two columns. With this correction, the calculation error caused by the model parameters in pentaquark calculation can be reduced partly. The results are analyzed in the following:

(a) $IJ^P = 0\frac{1}{2}^-$ (Table III); Single-color structure calculation shows that there exists two bound states in $\Xi\bar{K}^*$ and $\Xi^*\bar{K}^*$ channels while $\Xi\bar{K}$ and $\Omega\eta$ are unbounded. After coupling to the respective hidden-color channels, the binding energy of the two-bound states increase by a few MeVs. When coupled-channel calculations between both single-color structures and all type of structures is performed, the lowest energy is above the threshold of $\Xi\bar{K}$, so no bound state can be formed in the $IJ^P = 0\frac{1}{2}^-$ system. However,

resonances are possible because the strong attractions exist in both the $\Xi\bar{K}^*$ and $\Xi^*\bar{K}^*$ channels. Thus, the real-scaling method is required to identify resonances.

- (b) $IJ^P = 1\frac{1}{2}^-$ (Table IV); The results are similar to that of the $IJ^P = 0\frac{1}{2}^-$ system, there are bound states in the $\Xi\bar{K}^*$ and $\Xi^*\bar{K}^*$ channels and the other two channels are unbounded. The lowest eigenenergy of the channel-coupling calculation is above the threshold of $\Xi\bar{K}$, so no bound state found in the $IJ^P = 1\frac{1}{2}^-$ system. $\Xi\bar{K}^*$ and $\Xi^*\bar{K}^*$ are possible resonances.
- (c) $IJ^P = 0\frac{3}{2}^-$ (Table V); The single-channel calculations show that there exists a bounded state in the $\Xi^*\bar{K}^*$ channel, Moreover, the attraction increases after coupling to its hidden-color channel. Although the single-channel calculation shows that the state $\Xi^*\bar{K}$ is unbounded, the couple-channels calculations push the states below the threshold. The coupling of all color singlet-singlet channels find the lowest eigenenergy of the system is 2029 MeV, 6 MeV below the threshold, The full-channel coupling lowers the lowest eigenenergy to 2025 MeV, so a bound state (the main component is $\Xi^*\bar{K}$) can be formed after the channel

TABLE V. The results for system with $IJ^P = 0\frac{3}{2}^-$. [cc1: mixing of color singlet-singlet channels, cc2: mixing of all channels (units are in MeV).].

ψ^f_i	ψ^{σ_j}	ψ^{c_k}	Channel	E	$E_{\text{th}}^{\text{Theo}}$	E_B	$E_{\text{th}}^{\text{Exp}}$	E'
$i = 1$	$j = 6$	$k = 1$	$\Xi\bar{K}^*$	2232	2232	0	2207	2207
$i = 1$	$j = 6, 7$	$k = 1, 2, 3$		2232				
$i = 1$	$j = 8$	$k = 1$	$\Xi^*\bar{K}$	2035	2035	0	2028	2028
$i = 1$	$j = 8$	$k = 1, 3$		2035				
$i = 1$	$j = 9$	$k = 1$	$\Xi^*\bar{K}^*$	2413	2451	-38	2422	2384
$i = 1$	$j = 9$	$k = 1, 3$		2378		-73		2349
$i = 2$	$j = 8$	$k = 1$	$\Omega\eta$	2232	2232	0	0	2220
$i = 2$	$j = 8$	$k = 1, 3$		2232				
$i = 2$	$j = 9$	$k = 1$	$\Omega\omega$	2262	2262	0	0	2454
$i = 2$	$j = 9$	$k = 1, 3$		2262				
cc1					2029	-6		
cc2					2025	-10		

TABLE VI. The results for system with $IJ^P = 1\frac{3}{2}^-$. [cc1: mixing of color singlet-singlet channels, cc2: mixing of all channels (unit are in MeV).].

ψ^f_i	ψ^{σ_j}	ψ^{c_k}	Channel	E	$E_{\text{th}}^{\text{Theo}}$	E_B	$E_{\text{th}}^{\text{Exp}}$	E'
$i = 3$	$j = 6$	$k = 1$	$\Xi\bar{K}^*$	2232	2232	0	2207	2207
$i = 3$	$j = 6, 7$	$k = 1, 2, 3$		2232				
$i = 3$	$j = 8$	$k = 1$	$\Xi^*\bar{K}$	2035	2035	0	2028	2028
$i = 3$	$j = 8$	$k = 1, 3$		2035				
$i = 3$	$j = 9$	$k = 1$	$\Xi^*\bar{K}^*$	2444	2451	-7	2422	2415
$i = 3$	$j = 9$	$k = 1, 3$		2436		-15		2407
$i = 4$	$j = 8$	$k = 1$	$\Omega\pi$	1811	1811	0	1812	1812
$i = 4$	$j = 8$	$k = 1, 3$		1811				
$i = 4$	$j = 9$	$k = 1$	$\Omega\rho$	2440	2440	0	0	2447
$i = 4$	$j = 9$	$k = 1, 3$		2440				
cc1					1810	-1		
cc2					1809	-2		

coupling in the $IJ^P = 0\frac{3}{2}^-$ system, which is regarded as a good candidate for $\Omega(2012)$. Also, it is possible for $\Xi^*\bar{K}^*$ to form a resonance.

- (d) $IJ^P = 1\frac{3}{2}^-$ (Table VI); The results are again similar to that of the $IJ^P = 0\frac{3}{2}^-$ system. There is only one bound state, $\Xi^*\bar{K}^*$ in the single-channel calculation, and it is possible to become a resonance. In addition, the channel coupling leads to a bound state in the system. The lowest eigenenergy is 1810 MeV (color singlet-singlet channel coupling), or 1809 MeV (full channel coupling), 1 MeV or 2 MeV lower than the threshold of the lowest channel $\Omega\pi$, so there is a bound state for the $IJ^P = 1\frac{3}{2}^-$ system.

- (e) For $J^P = \frac{5}{2}^-, I = 0, 1$ (Tables VII and VIII); The results of these two systems are similar. There is no bound state and the conclusions are the same after full-channel coupling.

From the above results, one can see that the isoscalar and isovector states have similar behavior; generally the isovector states have a little higher energy than that of the corresponding isoscalar states. This fact infers that the states are molecular ones; the large separation between baryon and meson minimize the contribution from the pion exchange potential. In the following, we shall calculate the separations between quarks to verify the molecular picture of the state.

TABLE VII. The results for system with $IJ^P = 0\frac{5}{2}^-$. [cc1: mixing of color singlet-singlet channels, cc2: mixing of all channels (units are in MeV).].

ψ^f_i	ψ^{σ_j}	ψ^{c_k}	Channel	E	$E_{\text{th}}^{\text{Theo}}$	E_B	$E_{\text{th}}^{\text{Exp}}$	E'
$i = 1$	$j = 10$	$k = 1$	$\Xi^*\bar{K}^*$	2451	2451	0	2422	2422
$i = 1$	$j = 10$	$k = 1, 3$		2451				
$i = 2$	$j = 10$	$k = 1$	$\Omega\omega$	2262	2262	0	2454	2454
$i = 2$	$j = 10$	$k = 1, 3$		2262				
cc1					2262	0		
cc2					2262			

TABLE VIII. The results for system with $IJ^P = 1\frac{5}{2}^-$. [cc1: mixing of color singlet-singlet channels, cc2: mixing of all channels. (unit are in MeV).].

ψ^f_i	ψ^{σ_j}	ψ^{c_k}	Channel	E	$E_{\text{th}}^{\text{Theo}}$	E_B	$E_{\text{th}}^{\text{Exp}}$	E'
$i = 3$	$j = 10$	$k = 1$	$\Xi^*\bar{K}^*$	2451	2451	0	2422	2422
$i = 3$	$j = 10$	$k = 1, 3$		2447				
$i = 4$	$j = 10$	$k = 1$	$\Omega\rho$	2440	2440	0	2447	2447
$i = 4$	$j = 10$	$k = 1, 3$		2440				
cc1					2440	0		
cc2					2440			

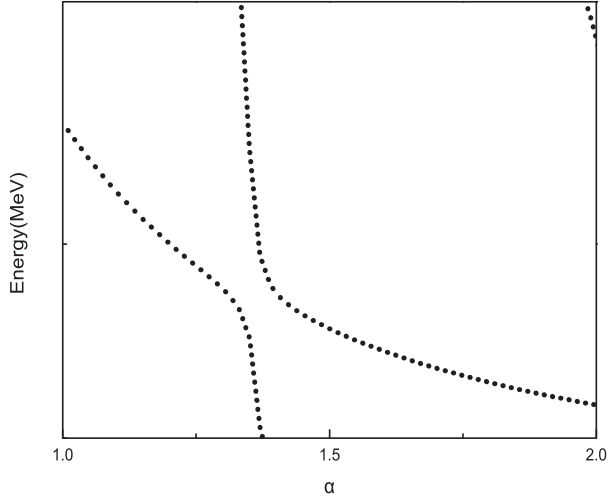
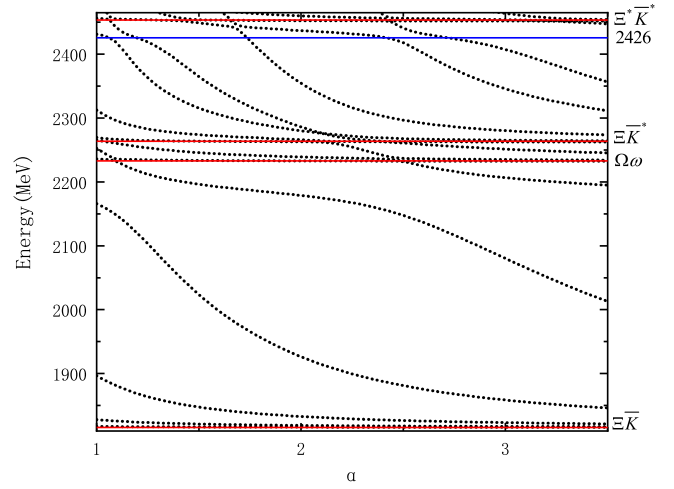
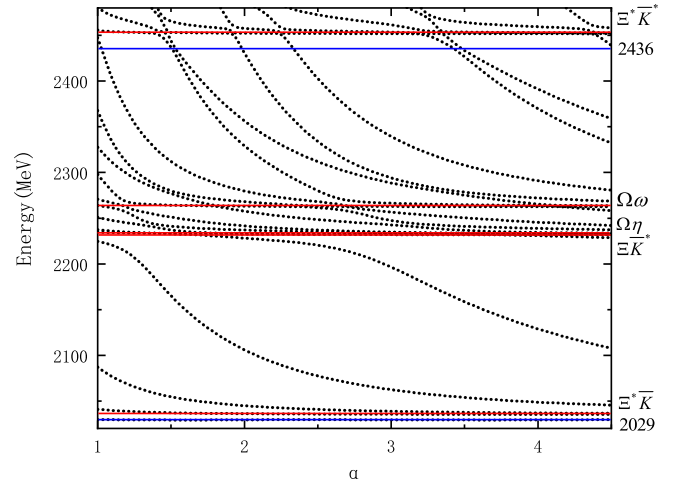
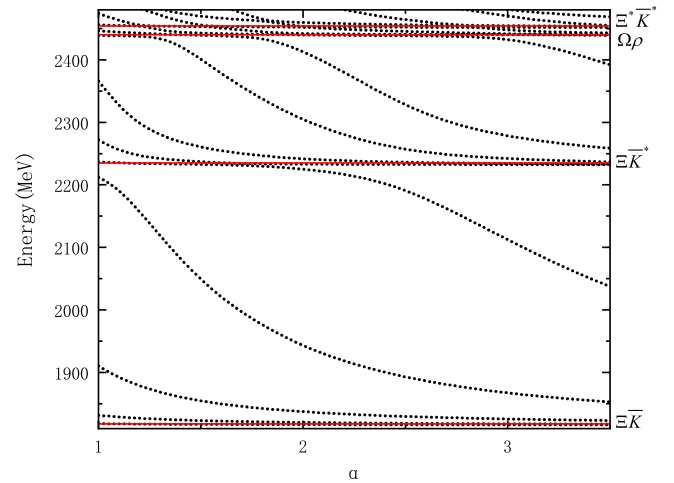


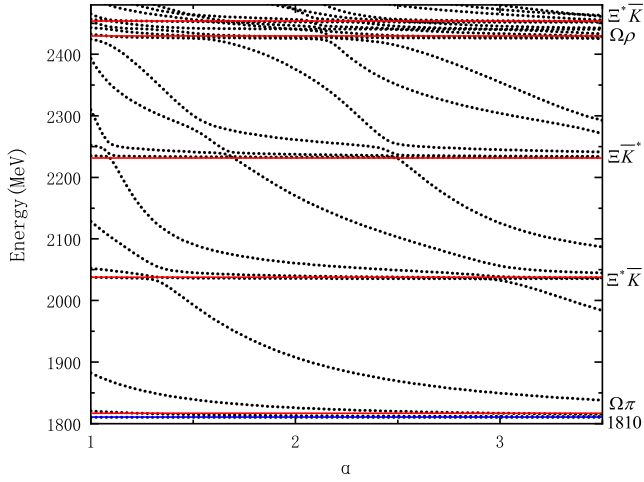
FIG. 1. The shape of the resonance in real-scaling method.

We make a comparison between our calculation results and that of Ref. [30]. The binding energies of states obtained in our work are generally bigger, basically on the order of tens since we consider the effects of scalar nonet exchange, whose contributions are strongly attractive and bind two hadrons together in our work. In Ref. [30], only the σ -exchange between nonstrange quarks is considered. For example, the binding energy of $[\Xi\bar{K}^*]_{0\frac{1}{2}^-}$ is 54 MeV, whereas it is 8 MeV in Ref. [30], and it is reasonable that $[\Xi^*\bar{K}^*]_{0\frac{1}{2}^-}$, $[\Xi\bar{K}^*]_{1\frac{1}{2}^-}$, and $[\Xi^*\bar{K}^*]_{1\frac{1}{2}^-}$ (with more than a dozen binding energies in our work) become unbound in Ref. [30]. For $IJ^P = 0\frac{3}{2}^-$ system, we solve the mass-inversion problem of $\Xi^*\bar{K}$ and $\Omega\eta$, which leads to a more objective description on the effect of channel coupling. Then, in the $IJ^P = 1\frac{3}{2}^-$ system, there is no mass-inversion problem in both of the two calculations, and we found that our results are consistent with those of Ref. [30]. Finally, for the $IJ^P = 0\frac{5}{2}^-$ and $1\frac{5}{2}^-$ systems, the results are the same in both of the calculations, and there is not any bound state.

To check whether the resonances in $IJ^P = 0\frac{1}{2}^-$, $0\frac{3}{2}^-$, $1\frac{3}{2}^-$ and $1\frac{3}{2}^-$ systems can survive after coupling to the open channels, a stability method to identify genuine resonance states, the real scaling method (stabilization method) [36–38], is employed. In this method, the Gaussian size parameter r_n , appearing in Eq. (13), for the basis functions between the color-singlet baryon and meson clusters is scaled by a factor of α : $r_n \rightarrow \alpha r_n$. As a result, a genuine resonance will act as an avoid-crossing structure (see Fig. 1) with the increasing of α , while other continuum states will fall off towards its threshold. If the avoid-crossing structure is repeated periodically as α increases, then the avoid-crossing structure is a genuine resonance.

Our results are shown in Figs. 2–5, and in these figures the thresholds of all physical channels appear as horizontal

FIG. 2. Energy spectrum of $0\frac{1}{2}^-$ system.FIG. 3. Energy spectrum of $0\frac{3}{2}^-$ system.FIG. 4. Energy spectrum of $1\frac{1}{2}^-$ system.

FIG. 5. Energy spectrum of $1\frac{3}{2}^-$ system.

lines and are marked with lines (red lines) along with their tagged contents, and for genuine resonances, which appear as avoid-crossing structure and are marked with blue lines. Bound states are also marked with blue lines below the lowest threshold of the systems. The continuum states fall off towards their respective threshold (red horizontal lines). For the $IJ^P = 0\frac{5}{2}^-, 1\frac{5}{2}^-$ systems, since there is no any bound state in single-channel calculations (which means no mechanism of forming resonances) we do not present the results of these two systems.

For the $IJ^P = 0\frac{1}{2}^-$ system, we get one resonance whose energy is 2426 MeV (the main component is $\Xi^* \bar{K}^*$). The other possible resonance, $\Xi \bar{K}^*$, decays strongly to the open channels and cannot form an avoid-crossing structure, so we do not think it is an observable resonance. In the $IJ^P = 0\frac{3}{2}^-$ system, there is only one resonance and its energy is 2436 MeV (the main component is $\Xi^* \bar{K}^*$) and there is also a bound state which lies below the lowest threshold (a blue line marked by 2029). Although there are two channels where weakly bound states exist in the single channel calculation for the $IJ^P = 1\frac{1}{2}^-$ system, we found no avoid-crossing structure, which means there is not any resonance. Finally, in the $IJ^P = 1\frac{3}{2}^-$ system, there is not any resonance. However, the lowest energy of this system is pushed below the lowest threshold of the system $\Omega\pi$ by the channel coupling, thus there is a bound state which is shown as a blue line marked by 1810. It is worth mentioning that in

case we use the real-scaling method to identify resonances and we will also calculate the composition of the possible resonances to find the mechanism of the formation of the resonances. The main component of a genuine resonance should be bound state channels in the single-channel calculation or coupled channels with energy below the lowest threshold of the coupling channels in the channel-coupling calculation. For example, in Fig. 5, there is an avoid-crossing structure around 2250 MeV. However, its main component is $\Omega\omega$, an open channel, which means the avoid-crossing structure is formed by two or more open channels which have different decreasing slopes.

For resonances, the partial widths of two-hadron strong decay can be extracted from these figures. The decay width of the resonance to possibly open channels of two hadrons is obtained by the following formula

$$\Gamma = 4V(\alpha) \frac{\sqrt{k_r k_c}}{|k_r - k_c|}, \quad (20)$$

where $V(\alpha)$ is the minimum energy difference, while k_c and k_r stand for the slopes of scattering state and resonance state, respectively (more details can be found in Ref. [36], and the total widths also include the decay width of each hadron in the pentaquark state. Bound states have no widths due to their stability against the strong decay. After a series of calculations and identification, we also calculate the root-mean-square distances between any two quarks in all bound states and observable resonances, respectively, to determine their inner structure and the results are shown in Table IX. The main component of each resonance and corrected energy are also given.

From Table IX, we can see that, for two resonances $\Omega(2426)$ and $\Omega(2436)$, the decay widths are 73.5 MeV and 68.4 MeV, respectively. The distances among quarks 1, 2, and 3 are 0.5–0.9 fm and the distances between quark 4 and antiquarks are 0.8–0.9 fm, while the distances between quarks 1, 2, 3, and 4, 5 are over 1.5 fm. Thus it is natural to describe these two resonances as molecular states. In addition, the distance of $\Omega(2426)$ between two clusters is obviously lower than that of $\Omega(2436)$ due to its higher binding energy of main component channel $\Xi^* \bar{K}^*$. For $\Omega(2029)$, the distances between quarks shows its structure is a molecular state. Also, the binding energy of the state in the single channel is 6 MeV and after coupling to

TABLE IX. The decay width and root-mean-square distances of Ω states in all systems.

Model	IJ^P	State	Main comp.	E'	Width	r_{12}	r_{13}	r_{14}	r_{15}	r_{34}	r_{35}	r_{45}
Resonance	$0\frac{1}{2}^-$	$\Omega(2426)$	$\Xi^* \bar{K}^*$	2396	73.5	0.7	0.9	1.5	1.6	1.6	1.6	0.9
	$0\frac{3}{2}^-$	$\Omega(2436)$	$\Xi^* \bar{K}^*$	2417	68.4	0.5	0.9	2.1	2.2	2.2	2.1	0.8
Bound state	$0\frac{3}{2}^-$	$\Omega(2029)$	$\Xi^* \bar{K}$	2018	...	0.7	0.8	2.3	2.3	2.3	2.3	0.5
	$1\frac{3}{2}^-$	$\Omega(1809)$	$\Omega\pi$	1810	...	0.7	0.7	3.5	3.5	3.5	3.5	0.5

TABLE X. Contributions of all potentials to the binding energy of $\Omega(2029)$ in $IJ^P = 0(\frac{3}{2})^-$ system (units are in MeV).

	Kinetic	Conf.	OGE	π	η	σ	a_0	f_0	$B.E$
$\Omega(2029)_{0\frac{3}{2}}$	15.0	-3.1	2.2	-0.9	-0.7	-14.2	-2.4	-1.5	-6

hidden-color channels, the binding energy increases by a few MeVs, which is the typical range of the binding energy of hadronic molecules. The corrected energy of molecular state $\Omega(2029)$ is 2018 MeV, close to 2012 MeV, so it is a good candidate for $\Omega(2012)$ reported by Belle Collaboration. Nevertheless, in the present work, we only consider all possible low-lying states of pentaquark systems with all orbital-angular momentums set to 0. Without this constraint, the state $\Omega(2029)$ can decay to D -waves $\Xi\bar{K}$ via the tensor interaction. So considering the effect of all possible D -wave channels is left for our further study. For $\Omega(1809)$, the result is similar to $\Omega(2029)$ and the structure of the state is a molecular one. However, the very small binding energy and the distance between two clusters of $\Omega(1809)$ is over 3 fm, which means it is a loose bound state.

To illustrate the mechanism of forming the $\Omega(2012)$ molecule, we further calculated the contributions from each term in the Hamiltonian and the results are shown in Table X. The values in the table are the differences between the contribution of each term in the pentaquark systems and the sum of its contribution in two individual hadrons. Here, the interactions of the kaon and kappa exchange do not work because the flavor wave function is based on SU(2) symmetry. From the table we can see that the main attractive interaction comes from the σ -meson exchange, which cancels the repulsive contribution of kinetic energy, and the Goldstone bosons and the corresponding scalar meson exchange are all attracted to bind the system. So the contributions of boson exchanges are dominant, which is consistent with the picture of $\Omega(2012)$ as a molecule. In addition, we calculated the components of channels in the state $\Omega(2029)$ to show the coupling strength between the main component $\Xi^*\bar{K}$ and other channels. The results show that the proportion of channel $\Xi\bar{K}^*$ and $\Omega\omega$ is very small and have no impact on forming the bound state. In addition, we calculated the components of channels in the state

$\Omega(2029)$ to show the coupling strength between the main component $\Xi^*\bar{K}$ and other channels. The results show that the other four channels reduce the energy of channel $\Xi^*\bar{K}$ by 6 MeV while the total proportion of the four channels is very small—less than 5%. The proportion of these four channels in descending order is $\Omega\eta$, $\Xi\bar{K}^*$, $\Xi^*\bar{K}^*$, and $\Omega\omega$, and their corresponding effects on forming binding energy are 4 MeV, 1 MeV, 1 MeV, and ~ 0 MeV, respectively.

IV. SUMMARY

In this work, all low-lying states of $sss\bar{q}q$, $q = u, d$ pentaquark systems are systematically investigated by means of the real-scaling method in the framework of the chiral quark model, with the help of a high-precision numerical approach, Gaussian expansion method.

The results show that $\Omega(2012)$ reported by Belle Collaboration can be described as $\Xi^*\bar{K}$ molecular state with $IJ^P = 0\frac{3}{2}^-$. In addition, a very loose bound state $\Omega(1810)$ with $IJ^P = 1\frac{3}{2}^-$ and two observable resonances, $\Omega(2396)$ and $\Omega(2417)$ with $IJ^P = 0\frac{1}{2}^-, 0\frac{3}{2}^-$ are found. The root-mean-square distances between any two quarks of these states are also calculated to determine their structures, along with their decay widths. The results shows that the four stable states are all molecular states. We hope the states proposed above can be searched in future experiments. Nevertheless, we cannot ignore the mixing of S - and D -wave of all states when the spin-orbit and tensor interactions are considered. So, further study is expected.

ACKNOWLEDGMENTS

The work is supported partly by the National Natural Science Foundation of China under Grants No. 11775118, and No. 11535005 and Postgraduate Research and Practice Innovation Program of Jiangsu Province under Grant No. KYCX22_1542.

- [1] J. Yelton *et al.* (Belle Collaboration), *Phys. Rev. Lett.* **121**, 052003 (2018).
[2] M. Gell-Mann, *Phys. Rev.* **125**, 1067 (1962).
[3] Y. Ne'eman, *Nucl. Phys.* **26**, 222 (1961).
[4] N. Isgur and G. Karl, *Phys. Rev. D* **18**, 4187 (1978).

- [5] S. Capstick and N. Isgur, *Phys. Rev. D* **34**, 2809 (1986); *AIP Conf. Proc.* **132**, 267 (1985).
[6] Y. Oh, *Phys. Rev. D* **75**, 074002 (2007).
[7] G. P. Engel, C. B. Lang, D. Mohler, and A. Schäfer (BGR Collaboration), *Phys. Rev. D* **87**, 074504 (2013).

- [8] J. L. Goity, C. Schat, and N. N. Scoccola, *Phys. Lett. B* **564**, 83 (2003).
- [9] L. Y. Xiao and X. H. Zhong, *Phys. Rev. D* **98**, 034004 (2018).
- [10] T. M. Aliev, K. Azizi, Y. Sarac, and H. Sundu, *Phys. Rev. D* **98**, 014031 (2018).
- [11] Z. Y. Wang, L. C. Gui, Q. F. Lü, L. Y. Xiao, and X. H. Zhong, *Phys. Rev. D* **98**, 114023 (2018).
- [12] E. E. Kolomeitsev and M. F. M. Lutz, *Phys. Lett. B* **585**, 243 (2004).
- [13] S. Sarkar, E. Oset, and M. J. Vicente Vacas, *Nucl. Phys.* **A750**, 294 (2005); **A780**, 90(E) (2006).
- [14] S. G. Yuan, C. S. An, K. W. Wei, B. S. Zou, and H. S. Xu, *Phys. Rev. C* **87**, 025205 (2013).
- [15] S. Q. Xu, J. J. Xie, X. R. Chen, and D. J. Jia, *Commun. Theor. Phys.* **65**, 53 (2016).
- [16] M. V. Polyakov, H. D. Son, B. D. Sun, and A. Tandogan, *Phys. Lett. B* **792**, 315 (2019).
- [17] F. K. Guo, C. Hanhart, U. G. Meissner, Q. Wang, Q. Zhao, and B. S. Zou, *Rev. Mod. Phys.* **90**, 015004 (2018).
- [18] M. P. Valderrama, *Phys. Rev. D* **98**, 054009 (2018).
- [19] R. Pavao and E. Oset, *Eur. Phys. J. C* **78**, 857 (2018).
- [20] Y. H. Lin and B. S. Zou, *Phys. Rev. D* **98**, 056013 (2018).
- [21] Y. Huang, M. Z. Liu, J. X. Lu, J. J. Xie, and L. S. Geng, *Phys. Rev. D* **98**, 076012 (2018).
- [22] S. Jia *et al.* (Belle Collaboration), *Phys. Rev. D* **100**, 032006 (2019).
- [23] N. Ikeno, G. Toledo, and E. Oset, *Phys. Rev. D* **101**, 094016 (2020).
- [24] J. X. Lu, C. H. Zeng, E. Wang, J. J. Xie, and L. S. Geng, *Eur. Phys. J. C* **80**, 361 (2020).
- [25] Y. H. Lin, F. Wang, and B. S. Zou, *Phys. Rev. D* **102**, 074025 (2020).
- [26] T. Gutsche and V. E. Lyubovitskij, *J. Phys. G* **48**, 025001 (2020).
- [27] M. S. Liu, K. L. Wang, Q. F. Lu, and X. H. Zhong, *Phys. Rev. D* **101**, 016002 (2020).
- [28] C. H. Zeng, J. X. Lu, E. Wang, J. J. Xie, and L. S. Geng, *Phys. Rev. D* **102**, 076009 (2020).
- [29] Belle Collaboration, arXiv:2207.03090.
- [30] X. J. Liu, H. X. Huang, J. L. Ping, and D. Y. Chen, *Phys. Rev. C* **103**, 025202 (2021).
- [31] E. Hiyama, Y. Kino, and M. Kamimura, *Prog. Part. Nucl. Phys.* **51**, 223 (2003).
- [32] X. H. Hu, Y. Tan, and J. L. Ping, *Eur. Phys. J. C* **81**, 370 (2021).
- [33] X. H. Hu and J. L. Ping, *Eur. Phys. J. C* **82**, 118 (2022).
- [34] G. Yang, J. L. Ping, and J. Segovia, *Phys. Rev. D* **102**, 054023 (2020).
- [35] Y. Tan and J. L. Ping, *Chin. Phys. C* **45**, 093104 (2021).
- [36] J. Simons, *J. Chem. Phys.* **75**, 2465 (1981).
- [37] E. Hiyama, A. Hosaka, M. Oka, and J. M. Richard, *Phys. Rev. C* **98**, 045208 (2018).
- [38] Q. Meng, E. Hiyama, K. U. Can, P. Gubler, M. Oka, A. Hosaka, and H. Zong, *Phys. Lett. B* **798**, 135028 (2019).
- [39] A. Valcarce, H. Garcilazo, F. Fernandez, and P. Gonzalez, *Rep. Prog. Phys.* **68**, 965 (2005).
- [40] H. Garcilazo, T. Fernandez-Carames, and A. Valcarce, *Phys. Rev. C* **75**, 034002 (2007).